LAWRENCE
LIVERMORE
NATIONAL
LABORATORY

LLNL-JRNL-822199

High-pressure stability of B-Zr: No evidence for isostructural phase transitions

E. F. OBannon, D. S. Sneed, P. Soderlind, M. J. Lipp, H. Cynn, J. S. Smith, C. Park, Z. Jenei

May 3, 2021

High Pressure Research

Disclaimer

High-pressure stability of β-Zr: No evidence for isostructural phase transitions

[1]E.F. O'Bannon III, [1]D.S. Sneed, [1]P. Söderlind, [1]M.J. Lipp, [1]H. Cynn, [2]J.S. Smith, [2]C. Park, and [1]Zs. Jenei

[1]Physics Division, Physical & Life Sciences Directorate, Lawrence Livermore National Laboratory, Livermore, CA 94550, USA

[2]High Pressure Collaborative Access Team, X-Ray Science Division, Argonne National Laboratory, Argonne, Illinois 60439, USA

Abstract

Isostructural transitions have been reported to occur in a small number of pure elements, however most of these either remain controversial or have been disproven. Zr is one of those elements which remains controversial with two reports of an isostructural bcc-to-bcc transition at ~56-60 GPa at ambient temperature and a more recent report proposing a second bcc-to-bcc transition at 110 GPa. Here we report a detailed experimental and theoretical study of zirconium in the pressure region of the proposed isostructural transition(s). We conducted three quasi-hydrostatic room temperature static compression experiments on three different purity Zr samples using Ne as a pressure transmitting medium up to 80 GPa. We observe that the α → ω transition pressure is inversely proportional with the sample purity which is consistent with previous work. We observed the ω → β transition to initiate at ~35 GPa in all three runs and we see no evidence for an isostructural transition finding a smooth compression curve from 35 to 80 GPa. We determined the theoretical volume as well as the following parameters C_{11}, C_{12}, C_{44}, bulk modulus, shear modulus, Young's modulus, and Poisson's ratio for β-Zr up to 717 GPa and no obvious anomalies are identified. Our new results join the growing body of evidence that does not find any indication of isostructural transitions in Zr compressed to high pressure at ambient temperature.

Introduction

Isostructural phase transitions in pure elements are extremely unusual. An fcc-to-fcc transition in Cs was reported to occur at ambient temperature near 4.2 GPa [1,2]. While a theoretical study at 0 K did not find any evidence of the isostructural transition they did suggest that thermal effects may play a role [3]. An X-ray diffraction study showed that Cs transforms to an orthorhombic phase above 4.2 GPa [4] and

no evidence of the fcc form was found. Akahama *et al.* [5] compressed Zr without a pressure transmitting medium (PTM) to 68 GPa and they report that above ~56 GPa the volume of Zr decreases discontinuously. They reported that "the anomaly may be an isostructural first-order transition." This volume discontinuity was not supported by theoretical studies, where instead a smooth compression curve through this region was predicted [6-8]. The calculated high-pressure elastic moduli and compression curves of β-Zr up to 72 GPa do not show any discontinuities in the pressure range of the reported isostructural transition [9,10]. In Ce an fcc-to-fcc phase transition occurs at ~0.7 GPa with an associated volume collapse of ~15%. This transition has been confirmed by many independent research groups who have reproduced these results experimentally [1,11-18]. Additionally, from a theoretical perspective the existence of the isostructural transition in Ce is no longer debated, only the driving mechanism remains controversial [19,20]. Very recently, Ji *et al.* [21] report isostructural electronic transitions in hydrogen at very high pressures, however this remains controversial [22] and has not yet been confirmed by other research groups.

A new high-pressure X-ray diffraction study of Zr [23] has reported to confirm the previous report by Akahama *et al.* [5] of an isostructural phase transition in Zr. Stavrou *et al.* [23] compressed Zr without a PTM at ambient temperature to 211 GPa and proposed an isostructural bcc-to-bcc transition with a volume change of 4% occurs between 57.5 to 60 GPa [23]. Their first-principles quantum-molecular-dynamics calculations support the existence of this transition and point to anharmonic effects as being the trigger for the transition. Pigott *et al.* [24] conducted quasi-hydrostatic and non-hydrostatic in situ X-ray diffraction experiments, and non-hydrostatic high-pressure electrical resistivity measurements and they did not observe the proposed isostructural transition in any of their experiments and they reported equation of state (EOS) parameters for β-Zr. Anzellini *et al.* [25] conducted quasi-hydrostatic X-ray diffraction experiments on Zr up to 142 GPa in a He PTM at ambient temperature and did not observe the proposed isostructural transition and found that β-Zr was stable to at least 142 GPa. They also verified their results with numerical heating-quenching experiments and found that there is no dynamical

instability due to a soft mode between 25 and 100 GPa. Following these more recent reports a study was published that was a reanalysis of the *P*-*V* data reported by Stavrou *et al.* [23] and a second bcc-to-bcc phase transition is proposed to occur near 110 GPa [26]. Gal [26] does not discuss the two recent quasi-hydrostatic diamond anvil cell studies [25] where the isostructural transition(s) were not observed.

We have conducted three quasi-hydrostatic Ne loaded high-pressure synchrotron X-ray diffraction experiments on Zr with different purities up to a maximum pressure of 80 GPa and we calculated the high-pressure elastic moduli, Poisson's ratio, and compression curve of β-Zr up to 717 GPa. The goal our experiments was to carefully examine under quasi-hydrostatic conditions the stability of β-Zr in the pressure range of the proposed isostructural phase transition with multiple experiments using Zr samples of different purities. Our purities bracket the purity of the sample used by Stavrou *et al.* [23] in order to evaluate if sample purity may play a role in the stability of β-Zr. We compare our new experimental and theoretical results with [9,10,23-26], and we discuss the existence of the proposed isostructural transition(s) in β-Zr.

Methods

High-Pressure X-ray diffraction measurements

Membrane diamond anvil cells [27] were equipped with 200 μm flat diamond anvils and Re gaskets. For all three experiments Re gaskets were pre-indented to ~30 μm and a ~100 μm diameter holes were drilled into the center to create the sample compartment. Zr and a pressure marker, either Au or W, were loaded into the sample compartment and Ne gas was loaded at 1.8 kbar using a high-pressure gas loader. Three runs were carried out using foil Zr samples. Run 1 Zr foil from Alfa Aesar with a purity of 99.94%, Run 2 Zr foil from ESPI metals with a purity of 99.9%, and Run 3 with a Zr foil from GoodFellow with a purity of 99.2%. The Au pressure marker used in all three runs was a powder obtained from Alfa Aesar with a grain size ranging from 0.8-1.5 μm with a purity of 99.9%. The W pressure marker used only in Run 1 was obtained from Alfa Aesar with a grain size ranging from 1-5 μm and a purity of 99.9 %.

Angle dispersive x-ray diffraction (ADXRD) experiments were carried out at the High-Pressure Collaboration Access Team (HPCAT) Run 1 was carried out on beamline 16ID-B while runs 2 & 3 were carried out on 16 BMD. At beamline 16 IDB a monochromatic X-ray beam of ~30 keV (λ = 0.4066 Å) was focused to a beam size of ~1x2 μm^2. Diffraction patterns were collected with a Pilatus 1M-F detector, with exposure times between 4 and 30 s. At beamline 16 BMD a monochromatic X-ray beam of ~25 keV (λ = 0.4959 Å) was focused to a beam size of ~4x7 μm^2. Diffraction patterns were collected with a MAR-345 image plate detector with exposure times up to 300 s. Sample positioning and centering was accomplished by the fly scan method [28] on both beamlines. Detector distance and orientation was calibrated using a CeO_2 standard for both beamlines.

The two-dimensional diffraction patterns were radially integrated using DIOPTAS [29] to obtain an intensity curve of the diffraction peaks as a function of the 2θ angle, which were analyzed to obtain peak positions using our in-house analysis codes in OriginPro software package. The pressure inside the high-pressure chamber of the DACs was estimated by measuring the unit cell volume of Ne [30]. We loaded Au in all three runs and W in run 1 however, due to peak overlap with Au and Zr we estimated the pressure in all three runs using the Ne (111) reflection so that the pressure estimation is consistent between all three runs. It should be noted that we found the pressure estimates from W [31] and Au [32] agreed well with the pressure estimate from the Ne with deviations of less than 0.25 GPa at the maximum pressure of each run. The volume of β-Zr was calculated from the (211) reflection since it did not overlap with the pressure marker or the PTM over the entire pressure range of these measurements. We found that when we calculated the volume from the β-Zr (110), (220), (211), or (310) the differences were close to the uncertainties of the volume calculation. Not surprisingly volumes calculated from the (200) reflection do show a deviation that is slightly larger than the uncertainties from the volumes calculated from the other reflections.

Evaluation of stress states

A line-shift analysis was performed in order to evaluate the pressurizing conditions in the Ne loaded sample for all three runs. The lattice parameter (cubic system) is obtained directly from the measured *d*-spacings and under nonhydrostatic conditions the measured lattice parameter systematically deviates from the hydrostatic value depending on the *hkl* indices [33,34]. While under hydrostatic conditions for the cubic system the lattice parameter is independent of *hkl* indices [33]. The uniaxial stress component *t* can be calculated using the following equation.

$$t \sim -3M_1/(\alpha M_0 S) \quad (1)$$

One can obtain *t* from the slope M_1 and the intercept M_0 of a plot of $a_m(hkl)$ versus $3(1-3\sin^2\theta)\Gamma(hkl)$ (termed the gamma plot) together with α and *S*. a_m is the measured lattice parameter and θ is half the Bragg angle of the reflection (*hkl*). α determines the relative weights of the isostress and isostrain conditions and we used a value of 1 for this analysis. The high-pressure elastic constants for β-Zr were calculated using density functional theory (DFT). The elastic anisotropy parameter *S* can be obtained with Eq. 2, which can be expressed by C_{ij} as

$$S = 1/(C_{11} - C_{12}) - 1/(2C_{44}) \quad (2)$$

In the axial diffraction geometry lattice parameters obtained under positive uniaxial stress are larger than the hydrostatic values, while those obtained under negative uniaxial stress are smaller [32,33]. The hydrostatic lattice parameter can be calculated and for a complete discussion including the derivation of all relevant equations we refer readers to the following references [33-35].

Computational Details

DFT calculations of β-Zr beyond 700 GPa utilizing an all-electron full-potential linear-muffin-tin orbitals (FPLMTO) method were carried out. This method does not rely on any core-electron assumption and approximations are few and numerical in nature, outside of the necessary electron-correlation functional. FPLMTO is fully relativistic and includes spin-orbit interaction, here applied only for the d and f states for best accuracy [36]. Details of the method and set-up parameters of the calculations were the

same as in our recent assessment of DFT for equation-of-state [37]. We employed the generalized gradient approximation (GGA) [38] for the electron exchange and correlation functional. The bulk shear, and Young's moduli and the Poisson's ratio were also calculated to 717 GPa. We used the Hill average for the shear modulus. For determining the elastic constants, we applied twenty volume-conserving strains each for the C' and the C_{44} moduli, then fitting a 4th-order polynomial to the total-energy response and extracting the coefficient for the 2nd-order term. For C' we assumed the conventional strain [39] while for C_{44} we followed the approach with a volume-preserving monoclinic strain as recommended for vanadium by Lee *et al.* [39]. We utilized many k points (3000-8000) to ensure good resolution of the small energy differences associated with the small strains (1-2%).

Results and Discussion

In all three experimental runs we collected data across the α → ω transition and while this work is primarily focused on the stability of β-Zr it is worth discussing the α → ω transition pressure observed in these runs. Velisavljevic *et al.* [40] reported that the α → ω transition pressure increases with the amounts of interstitial impurities. Under hydrostatic conditions the α → ω transition in high purity Zr initiates at 6.4 GPa while in Zr with significant interstitial impurities (e.g. impurities in ppm include Hf=14000; Fe=2400; O=1200) the α → ω transition initiates at a 11.6 GPa [40]. For our three studied samples we observe an increase in the transition pressure as the sample purity decreases (See Table I for transition pressures for each run). Akahama *et al.* [5] reported that they observe this transition to occur at 6.7 GPa and that their sample was 99.8% pure, but there is a very large gap between the last α -Zr and first ω -Zr as seen on their figure 2. Stavrou *et al.* [23] used a 99.5% pure Zr sample and they reported the α → ω transition to occur at ~12.7 GPa. Anzellini *et al.* [25] used both 99.2 and 98.8 % purity and they reported that the α → ω transition occurred between 14-20 GPa. These data all confirm the trend of a higher α → ω transition pressure with lower purity Zr reported by Velisavljevic *et al.* [40]. Interestingly, all experimentally determined transition pressures are higher than the pressure determined from *Ab initio*

calculations where they find at 300 K the α → ω transition occurs at 1.7 GPa [41]. This may indicate that even in high purity Zr there are still enough impurities to impede grain growth of ω-Zr. This may delay the formation of large enough domains of ω-Zr such that the onset pressure as determined by X-ray diffraction appears higher than it is in Zr with absolutely zero impurities.

The ω → β transition was observed to initiate at ~35 GPa in all three runs (see Table I for exact pressures for each run). Xia *et al.* [42] report that this transition occurs at 30±2 GPa. Akahama *et al.* [5] reported that they observe this transition to occur at 33 GPa. Stavrou *et al.* [23] reported the ω → β transition to occur at ~30 GPa. Pigott *et al.* [24] reported that this transition completes by ~37 GPa in their quasi-hydrostatic experiment and that it occurs at 35 GPa in their non-hydrostatic electrical resistivity measurements. Anzellini *et al.* [25] report that they observe the ω → β transition to occur at 35 GPa in their experimental runs. While DFT calculations predict this transition to be lower than experimentally observed at 27-28 GPa [43,44].

The β-Zr compression curves measured in all three experimental runs from this study show no discontinuities between 35 and 80 GPa (Fig 1). Our quasi-hydrostatic results agree with the quasi-hydrostatic results of Pigott *et al.* [24] and Anzellini *et al.* [25] who also report that they do not see any evidence of discontinuities in their β-Zr compression curves. The measured volumes of β-Zr and pressure from all three runs are shown in Table II. Interestingly, while the Akahama *et al.* [5] results are more scattered than ours on average they agree with our compression curve. Moreover, Akahama *et al.* [5] proposed that an isostructural transition with a ~1% change in volume may occur at 56 GPa. However, their measured *P*-*V* data is scattered on the order of ~1% which was noted by Anzellini *et al.* [25]. Akahama *et al.* [5] used Au as their PTM while Au is known to sustain very low uniaxial stress at high pressure [45] the pressurizing conditions in an Au PTM are not ideal. The results of Pigott *et al.* [24] are different by ~3% between their two reported quasi-hydrostatic runs. Their quasi-hydrostatic run up to 69 GPa deviates from all three of our runs and the results of Anzellini *et al.* [25] and this is likely due to this run not having

enough He PTM in the sample chamber (See Pigott *et al.* [24] Fig. 1a) which was also noted by Anzellini *et al.* [25].

The difference in the Stavrou *et al.* [23] and Xia *et al.* [42] *P-V* data and the results of this present study and Akahama *et al.* [5], Pigott *et al.* [24], and Anzellini *et al.* [25] is obvious. Both their *P-V* curves plot below our new results and the results of [5,24,25]. Moreover, the Stavrou *et al.* [23] results appear "wavy" where portions of the *P-V* curve appear to show the sample volume increasing as the pressure increases and they are not scattered in the same way the results of Akahama *et al.* [5] are (see Stavrou *et al.* [23] Fig. 1). They also report that an isostructural transition from β-Zr to β'-Zr occurs between 57.5-60 GPa with a volume change of 4%. If either their pressure estimation or volume estimations are systematically off, it could explain why their *P-V* curve is shifted from these new results and [5,24,25]. We find that near the proposed isostructural transition a ΔV of +0.45 Å^3, or a ΔP of +6.0 GPa would shift their curve to be in better agreement with our new results. However, the uncertainty in volume measured by ADXRD cannot explain this discrepancy (which was also noted by Anzellini *et al.* [25]), and therefore, the pressure estimation is likely the culprit here.

We came to the same conclusion as Anzellini *et al.* [25] did, based on supplementary figure S1 reported by Stavrou *et al.* [23], there was a pressure difference between the sample and the pressure marker. They show several diffraction patterns that contain only reflections from β-Zr with no signal from their Au pressure marker. In our quasi-hydrostatic experiments, the Au (111) and β-Zr (110) reflections cannot be deconvolved from each other above ~70 GPa. In the non-hydrostatic experiments of Akahama *et al.* [5] and Stavrou *et al.* [23] these two reflections would begin to overlap at lower pressures due to peak broadening from the non-hydrostatic loading conditions. Therefore, at least within the pressure range of the proposed isostructural transition they must have moved to a different spot in the sample chamber to obtain a diffraction pattern that only contained Au. Depending on the beam focus this was at least a few micrometers away and possibly even up to 10's of micrometers away. Stavrou *et al.* [23]

assumed that since Zr has sufficient plasticity it can be considered intrinsically hydrostatic. However, non-hydrostatic stress is limited by the yielding of the sample, and it has been shown that pressure gradients in the DAC can reach several GPa/µm [46,47]. There was most likely a relatively large pressure difference between the sample and the pressure marker in the experiments reported by Stavrou *et al.* [23]. We speculate that the pressure marker recorded a lower pressure than the sample was under. We note that the choice of Au EOS could also have played a role. However, since Stavrou *et al.* [23] did not report the Au EOS they used for pressure estimation we cannot investigate this further.

The results of Xia *et al.* [42] can likely be explained by their experimental approach, they performed two experiments. In their experiment 1 they used Au as their pressure marker using the calibration reported by Jamieson *et al.* [48] and measured the volume of Zr up to some unknown pressure. In their experiment 2 they measured only Zr to avoid peak overlap between Zr and Au and estimated the pressure from the measured Zr EOS from their first experiment. Xia et al. [42] show in their Figure 1 diffraction patterns with only Zr reflections which were collected from experiment 2. In the pressure range where we observe the ω → β transition (35 GPa) the pressure estimated from Au at a volume of 14.728 $Å^3$ from the following EOS's are 34.7 GPa using Jamieson *et al.* [48], 35.7 GPa Fei *et al.* [49], 35.5 GPa Takemura and Dewaele [32], and 35.0 GPa Yokoo *et al.* [50]. Therefore, their choice of Au EOS cannot fully explain their shifted *P-V* curve which appears to be ~5.0 GPa lower than our results. Therefore, it is likely that the measured Zr EOS obtained from their experiment 1 underestimated the pressure by ~4-5 GPa at the ω → β transition and that the uncertainties in pressure they report are likely larger.

Additional evidence that the pressure was underestimated by [23,42] can be found when considering that X-ray diffraction data collected in the axial geometry under non-hydrostatic conditions are shifted from those measured under hydrostatic conditions [33-35,51,52]. When no PTM is used the measured volumes are larger than when a soft PTM is used [34,52]. Therefore, under non-hydrostatic conditions the pressure will be underestimated when using a hydrostatic EOS for pressure determination.

The *P*-*V* curve under these conditions would shift above where it would be found under hydrostatic conditions (appearing stiffer) which is the opposite of what we find when comparing our new results to [23,42]. Therefore, non-hydrostatic conditions alone cannot explain these shifted *P*-*V* curves, and this further supports our hypothesis that the pressure marker was at a lower pressure than the sample in the experiment(s) reported by [23].

Any equation of state (EOS) parameters that are obtained from fits to non-hydrostatic data will be biased [52,53]. The presence of non-hydrostatic conditions can be detected using the line shift analysis and the magnitude of *t* can be estimated [35]. Non-hydrostatic conditions can be corrected for using the line-shift approach [33,51] and EOS parameters obtained from the corrected results agree well with those obtained under quasi-hydrostatic conditions [34,54]. There are limitations to this approach, however, that are discussed in detail elsewhere [35,55]. We fit the β-Zr results from all three runs with a Vinet EOS [56] and we show the results of these fits in Table III. β-Zr EOS parameters from the fit are V_0 (ambient volume), K_0 (ambient isothermal bulk modulus) and K'_0 (the first pressure derivative of the bulk modulus). Our obtained Vinet EOS parameters agree well with those reported by Anzellini *et al.* [25]. We find that parameters obtained from Vinet fits to the *P*-*V* data from run 3 deviate from those obtained from fits to runs 1 and 2. This was probably because the pressurizing conditions were different in run 3 which will be discussed in more detail below. We fit to the β-Zr data reported by Stavrou *et al.* [23] with a Vinet EOS and found that β-Zr is more compressible in their study which is the opposite of what one would expect to find under non-hydrostatic conditions. We re-fit the quasi-hydrostatic run from Pigott *et al.* [24] that likely had the best pressurizing conditions (see their Fig 1b). However, their results appear stiffer than ours and those of Anzellini *et al.* [25].

In Fig. 2 we show diffraction patterns from run 1 specifically in the pressure region of the proposed isostructural transition where the sample, pressure marker, and PTM are measured at the same spot in the high-pressure chamber, so we are confident that the sample and pressure marker are at the same

pressure. We do not observe any sudden changes or discontinuous shifts of any of the resolved reflections from β-Zr, and we do not observe any new reflections that may indicate a phase transition across the pressure range of these measurements. In Fig. 3 we show the *d*-spacings as a function of pressure from run 1 for the β-Zr (110), (200), (211), (220), and (310) reflections from 50 to 70 GPa and no discontinuities are observed. We also do not observe discontinuities in the *d*-spacings as a function of pressure in runs 2 or 3 either. Furthermore, we find no evidence in our 3 experimental runs with different purities of Zr samples for the isostructural β → β' transition proposed by Stavrou *et al.* [23]. Our new results are in accord with the recent studies of Pigott *et al.* [24] and Anzellini *et al.* [25] who also report that they do not observe an isostructural β → β' transition in this pressure range.

Theoretically we examined volume-compression behavior of β-Zr and calculated within DFT the following parameters under compression to 717 GPa: C_{11}, C_{12}, C_{44}, (Figure 4) and the bulk modulus, shear modulus, Young's modulus, and Poisson's ratio (Figure 5). These calculated values are shown in Table IV. The previous studies of Wang *et al.* [9] and Zhang *et al.* [10] also reported these parameters but were limited in pressure to 60 and 72 GPa respectively. Discontinuities or kinks are not observed in our newly calculated high-pressure elastic moduli or Poisson's ratio (Figure 4 and 5) in the pressure range of the proposed β → β' transition (57.5-60 GPa) consistent with the results reported by [9,10]. Our calculated higher pressure results also do not show any anomalies in the pressure range of the proposed second isostructural transition β' → β" at 110 GPa. We predict a smooth compression curve for β-Zr up to 717 GPa. Our new theoretical results agree well with Zhang *et al.* [10] while the bulk modulus, Poisson's ratio, and C_{12} reported by Wang *et al.* [9] shows the most obvious disagreement between this study and Zhang *et al.* [10]. Present calculations are more accurate than either [9,10] because those studies relied on the pseudopotential approximation. This computationally efficient way of dealing with the core electrons in a metal is increasingly inaccurate with compression. The C_{12} moduli by Wang *et al.* [9] is different than that of Zhang *et al.* [10] and our present theory which is likely due to their inaccurate calculation of the

bulk modulus, see figure 5. Their bulk modulus [9] is far smaller than what Zhang *et al.* [10] and we calculate. Since for cubic materials C_{12} is calculated using $K = 1/3\ (C_{11} + 2C_{12})$ if K is low, it follows that also C_{12} will be low. The differences seen in figure 5d for the Poisson's ratio can also be explained in the same way as C_{12}.

We compared the theoretical results for K to our experimental results by calculating the isothermal bulk modulus from our fitted EOS and directly from our P-V data using $K_T = -V\ \partial P/\partial V$. The second approach does not rely on any assumptions with respect to the analytical form of the chosen EOS. For the direct calculation we fit our P-V data from run 1 with a spline interpolation and smoothing to mediate unphysical fluctuations similar to the approach described by [57]. The isothermal bulk moduli obtained from our the Vinet fit, and the direct calculation agree well with our new calculated results and those reported by Zhang *et al.* [10] figure 5a. This suggests that the calculated high pressure bulk moduli reported by Wang *et al.* [9] are inaccurate and too small.

We evaluated the stress state of our sample from all three runs across the pressure region where β-Zr is stable (35-80 GPa) using the line shift approach described above to calculate the uniaxial stress as described by [33,34,51]. Using our newly calculated elastic constants reported here, we show in Fig. 6 that the uniaxial stress sustained by β-Zr is low and is consistent with the uniaxial stress reported by Anzellini *et al.* [25]. These low values with no discontinuities or sudden changes in slope indicate that there is no sudden change in the pressurizing conditions in all three runs (e.g. PTM leaking out and sample becoming compressed directly between the diamonds). Interestingly, in run 3 the sustained uniaxial stress is higher than runs 1 and 2 showing that while all three samples were compressed in a Ne PTM that there can be differences in the pressurizing conditions between different runs and that evaluating the stress state of DAC experiments is a critical step in evaluating the reliability of the data. As mentioned above the parameters obtained from our Vinet fits to the P-V data from run 3 are as much as 3.7 % smaller for K_0 and 3.8% larger for K'_0. This is not surprising since the sustained uniaxial stress in run 3 was higher which

suggests that the stress state of the sample is different than in runs 1 and 2. Since our measured results from run 3 agree quite well with runs 1 and 2 and there is no discontinuous shift in the *P-V* curve it is unlikely that the PTM escaped. It is possible that the sample was compressed between the diamonds or pinched by the gasket with the sample remaining mostly in contact with the Ne PTM.

While the shifted *P-V* data can be explained as discussed above, an explanation for the proposed isostructural transition reported by Stavrou *et al.* [23] is more elusive. We studied a range of sample purities that bracket the sample purity reported by Stavrou *et al.* [23]. While Pigott *et al.* [24] used ultra-high purity Zr [58], and Anzellini *et al.* [25] used two samples with purities lower than those used by Stavrou *et al.* [23]. Thus, sample purity cannot reasonably explain why Stavrou *et al.* [23] observed an isostructural transition. Anzellini *et al.* [25] discuss possible changes in stress distribution during compression due to deformation of the diamond anvils (e.g. cupping of the anvils under high load). The pressure-load curve and deformation of typical flat and beveled diamond anvils is "s" shaped and can be divided into three stages with stage I and III having slower loading rates than stage II [59,60]. Stress redistribution occurs between stages II and III which is also where large scale cupping begins [60] and the pressure where this occurs depends on the culet diameter as well as DAC design, friction in the DAC assembly, and gasket material. We agree with Anzellini *et al.* [25] that that the proposed isostructural transition could be an artifact resulting from the deformation of the diamond anvils during different loading stages, most likely during the transition from loading stage II to loading stage III.

Recently Gal [26] refit the Zr *P-V* data reported by Stavrou *et al.* [23] with both Vinet [56] and Birch Murnaghan (BM) [61,62] equation of state forms and propose that another isostructural transition occurs at ~110 GPa the β' → β". These results do not agree with the recent quasi-hydrostatic results of Anzellini *et al.* [25] where they report that no discontinuities are observed between 35 and 142 GPa. Our new theoretical results, in terms of elastic constants, do not find any evidence for this proposed transition up to at least 717 GPa (see figures 4 and 5). Gal [26] state with respect to the DAC experiments reported

by Stavrou *et al.* [23] that "The use of fine powder of Zr as PTM remove uniaxial stress and possible misleading EOS." As discussed above, this statement contradicts what is known to happen to materials compressed non-hydrostatically in a DAC, and how non-hydrostatic conditions will bias obtained EOS parameters if they are not evaluated and corrected. Moreover, the choice of EOS by Gal [26] seems to be arbitrary as there is no explanation why Gal [26] chose a Vinet for some phases and a BM for other phases. Gal [26] does not address the differences between their new analysis of the Stavrou *et al.* [23] data and the recent reports of Pigott *et al.* [24] and Anzellini *et al.* [25], and Gal [26] does not cite these more recent studies. We discussed above and Anzellini *et al.* [25] also noted that the *P*-*V* data reported by Stavrou *et al.* [23] is probably somewhat inaccurate. Therefore, we suggest that any re-analysis of these *P*-*V* data should be considered flawed.

Concluding remarks

Our experimental and theoretical results join a body of work that does not find evidence of an isostructural transition in Zr at ~56-60 GPa at room temperature [6-10,24,25]. Additionally, the previous work of Anzellini *et al.* [25] and our new theoretical results see no evidence for the second isostructural transition at ~110 GPa proposed by Gal [26]. We speculate that non-hydrostatic compression effects combined with pressure measurement at a different location from the sample, and deformation of the diamond anvil during different stages of compression, explains the shifted *P*-*V* curve and the observation of the isostructural transition reported by Stavrou *et al.* [23]. Therefore, our data suggest that Ce remains the only pure element known to date where an isostructural phase transition has been unambiguously shown to occur.

Acknowledgments

This work was performed under the auspices of the US Department of Energy by Lawrence Livermore National Laboratory under Contract No. DE-AC52-07NA27344 and was supported in part by the LLNL-LDRD program under project No. 17-ERD-038. Portions of this work were performed at HPCAT

(Sector 16), Advanced Photon Source (APS), Argonne National Laboratory. HPCAT operations are supported by DOE-NNSA's Office of Experimental Sciences. The Advanced Photon Source is a U.S. Department of Energy (DOE) Office of Science User Facility operated for the DOE Office of Science by Argonne National Laboratory under Contract No. DE-AC02-06CH11357.

References

[1] P.W. Bridgman, Proceedings of the American Academy of Arts and Sciences **62**, 207 (1927).
[2] H.T. Hall, J.D. Barnett, and L. Merrill, Science **146**, 1297 (1964).
[3] D. Glotzel and A.K. McMahan, Physical Review B **20**, 3210 (1979).
[4] M.I. McMahon, R.J. Nelmes, and S. Rekhi, Physical Review Letters **87**, 255502 (2001).
[5] Y. Akahama, M. Kobayashi, and H. Kawamura, Journal of the Physical Society of Japan **60**, 3211 (1991).
[6] G. Jyoti and S.C. Gupta, Journal of Physics-Condensed Matter **6**, 10273 (1994).
[7] C.W. Greeff, Modelling and Simulation in Materials Science and Engineering **13**, 1015 (2005).
[8] S.A. Ostanin and V.Y. Trubitsin, Physica Status Solidi B-Basic Research **201**, R9 (1997).
[9] B.T. Wang, P. Zhang, H.Y. Liu, and W. D. Li, Journal of Applied Physics **109**, 063514 (2011).
[10] S.H. Zhang, X.Y. Zhang, Y. Zhu, S.L. Zhang, L. Qi, and R.P. Liu, Computational Materials Science **61**, 42 (2012).
[11] F. Decremps L. Belhadi, D.L. Farber, K.T. Moore, F. Occelli, M. Gauthier, A. Poliam, D. Antonangeli, C.M. Aracne-Ruddle, and B. Amadon, Physical Review Letters **106**, 065701 (2011).
[12] M.J. Lipp, D. Jackson, H. Cynn, C. Aracne, W.J. Evans, and A.K. McMahan, Physical Review Letters **101**, 165703 (2008).
[13] K.T. Moore, L. Belhadi, F. Decremps, D.L. Farber, J.A. Bradley, F. Occelli, M. Gauthier, A. Polian, and C.M. Aracne-Ruddle, Acta Materialia **59**, 6007 (2011).
[14] J. S. Olsen, L. Gerward, U. Benedict, and J. P. Itie, Physica B & C **133**, 129 (1985).
[15] M.N. Pavlovskii, V.V. Komissarov, and A.R. Kutsar, Combustion Explosion and Shock Waves **35**, 88 (1999).
[16] M.J. Lipp, A.P. Sorini, J. Bradley, B. Maddox, K.T. Moore, H. Cynn, T.P. Devereaux, Y. Xiao, P. Chow, and W.J. Evans, Physical Review Letters **109**, 195705 (2012).
[17] M.J. Lipp, Y. Kono, Zs. Jenei, H. Cynn, C. Aracne-Ruddle, C. Park, C. Kenney-Benson, and W.J. Evans, Journal of Physics-Condensed Matter **25**, 345401 (2013).
[18] M.J. Lipp, Zs. Jenei, H. Cynn, Y. Kono, C. Park, C. Kenney-Benson, and W.J. Evans, Nature Communications **8**, 1198 (2017).
[19] J.W. Allen and R.M. Martin, Physical Review Letters **49**, 1106 (1982).
[20] B. Johansson, Philosophical Magazine **30**, 469 (1974).
[21] C. Ji, B. Li, W. Liu, J.S. Smith, A. Majumdar, W. Luo, R. Ahuja, J. Shu, J. Wang, S. Sinogeikin, Y. Meng, V. B. Prakapenka, E. Greenberg, R. Xu, X. Huang, W. Yang, G. Shen, W.L. Mao, and H-K. Mao, Nature **573**, 558 (2019).
[22] L. Dubrovinsky, N. Dubrovinskaia, and M. I. Katsnelson, arXiv:1910.10772 (2019).
[23] E. Stavrou, L.H. Yang, P. Söderlind, D. Aberg, H.B. Radousky, M.R. Armstrong, J.L. Belof, M. Kunz, E. Greenberg, V.B. Prakapenka, and D.A. Young, Physical Review B **98**, 220101 (2018).
[24] J.S. Pigott, N. Velisavljevic, E.K. Moss, D. Popov, C. Park, J.A. Van Orman, N. Draganic, Y.K. Vohra, and B.T. Sturtevant, Journal of Physics-Condensed Matter **32**, 12lt02 (2020).

[25] S. Anzellini, F. Bottin, J. Bouchet, and A. Dewaele, Physical Review B **102**, 184105 (2020).
[26] J. Gal, Physica B: Condensed Matter **613**, 412979 (2021).
[27] Zs. Jenei, H. Cynn, K. Visbeck, and W.J. Evans, Review of Scientific Instruments **84**, 095114 (2013).
[28] J.S. Smith, E.A. Rod, and G. Shen, Review of Scientific Instruments **90**, 015116, 015116 (2019).
[29] C. Prescher and V.B. Prakapenka, High Pressure Research **35**, 223 (2015).
[30] A. Dewaele, F. Datchi, P. Loubeyre, and M. Mezouar, Physical Review B **77**, 094106 (2008).
[31] A. Dewaele, P. Loubeyre, and M. Mezouar, Physical Review B **70**, 094112, 094112 (2004).
[32] K. Takemura and A. Dewaele, Physical Review B **78**, 13, 104119 (2008).
[33] A.K. Singh, Journal of Applied Physics **73**, 4278 (1993).
[34] A.K. Singh and T. Kenichi, Journal of Applied Physics **90**, 3269 (2001).
[35] A.K. Singh, Journal of Physics and Chemistry of Solids **65**, 1589 (2004).
[36] B. Sadigh, A. Kutepov, A. Landa, and P. Soderlind, Applied Sciences-Basel **9**, 5020 (2019).
[37] P. Söderlind and D. A. Young, Computation **6**, 13 (2018).
[38] J.P. Perdew, *Electronic structure of solids '91* (Akademie Verlag, Berlin, 1991).
[39] B. Lee, R.E. Rudd, J.E. Klepeis, P. Söderlind, and A. Landa, Physical Review B **75**, 4, 180101 (2007).
[40] N. Velisavljevic, G.N. Chesnut, L.L. Stevens, and D.M. Dattelbaum, Journal of Physics-Condensed Matter **23**, 125402 (2011).
[41] Y.-J. Hao, L. Zhang, X.-R. Chen, L.-C. Cai, Q. Wu, and D. Alfe, Physical Review B **78**, 134101 (2008).
[42] H. Xia, S.J. Duclos, A.L. Ruoff, and Y.K. Vohra, Physical Review Letters **64**, 204 (1990).
[43] I. Schnell and R.C. Albers, Journal of Physics-Condensed Matter **18**, 1483 (2006).
[44] A. Landa, P. Söderlind, and P.E.A. Turchi, Journal of Alloys and Compounds **478**, 103 (2009).
[45] T.S. Duffy, G.Y. Shen, J.F. Shu, H.K. Mao, R.J. Hemley, and A.K. Singh, Journal of Applied Physics **86**, 6729 (1999).
[46] C. Meade and R. Jeanloz, Journal of Geophysical Research-Solid Earth and Planets **93**, 3261 (1988).
[47] R. M. Vignes, R. Becker, J. Stolken, and M. Kumar, Journal of Applied Physics **113**, 213503 (2013).
[48] J.C. Jamieson, J.N. Fritz, and M.H. Manghnani, in *High-pressure research in geophysics (Advances in Earth and Planetary Sciences 12)*, edited by A. S., and M. M.H. (Center for Academic Publications, Tokyo, 1982), pp. 27.
[49] Y. Fei, A. Ricolleau, M. Frank, K. Mibe, G. Shen, and V. Prakapenka, Proceedings of the National Academy of Sciences of the United States of America **104**, 9182 (2007).
[50] M. Yokoo, N. Kawai, K. G. Nakamura, K. Kondo, Y. Tange, and T. Tsuchiya, Physical Review B **80**, 104114, 104114 (2009).
[51] A.K. Singh, C. Balasingh, H.K. Mao, R.J. Hemley, and J.F. Shu, Journal of Applied Physics **83**, 7567 (1998).
[52] A. Dewaele and P. Loubeyre, High Pressure Research **27**, 419 (2007).
[53] K. Takemura, Journal of the Physical Society of Japan **76**, 202 (2007).
[54] E.F. O'Bannon, M.J. Lipp, J.S. Smith, Y. Meng, P. Soderlind, D.A. Young, and Zs. Jenei, Journal of Applied Physics **129**, 125901 (2021).
[55] A.K. Singh, Journal of Applied Physics **106**, 043514 (2009).
[56] P. Vinet, J. Ferrante, J.R. Smith, and J.H. Rose, Journal of Physics C-Solid State Physics **19**, L467 (1986).
[57] A.S.J. Mendez, F. Trybel, R.J. Husband, G. Steinle-Neumann, H-P. Liermann, and H. Marquardt, Physical Review B **103**, 064104 (2021).
[58] P.A. Rigg, C.W. Greeff, M.D. Knudson, G.T. Gray, and R.S. Hixson, Journal of Applied Physics **106**, 123532 (2009).

[59] B. Li, C. Ji, W. Yang, K. Yang, R. Xu, W. Liu, Z. Cai, J. Chen, and H-K. Mao, Proceedings of the National Academy of Sciences of the United States of America **115**, 1713 (2018).
[60] W.C. Moss and K. A. Goettel, Applied Physics Letters **50**, 25 (1987).
[61] F.D. Murnaghan, Proceedings of the National Academy of Sciences of the United States of America **30**, 244 (1944).
[62] F. Birch, Physical Review **71**, 809 (1947).

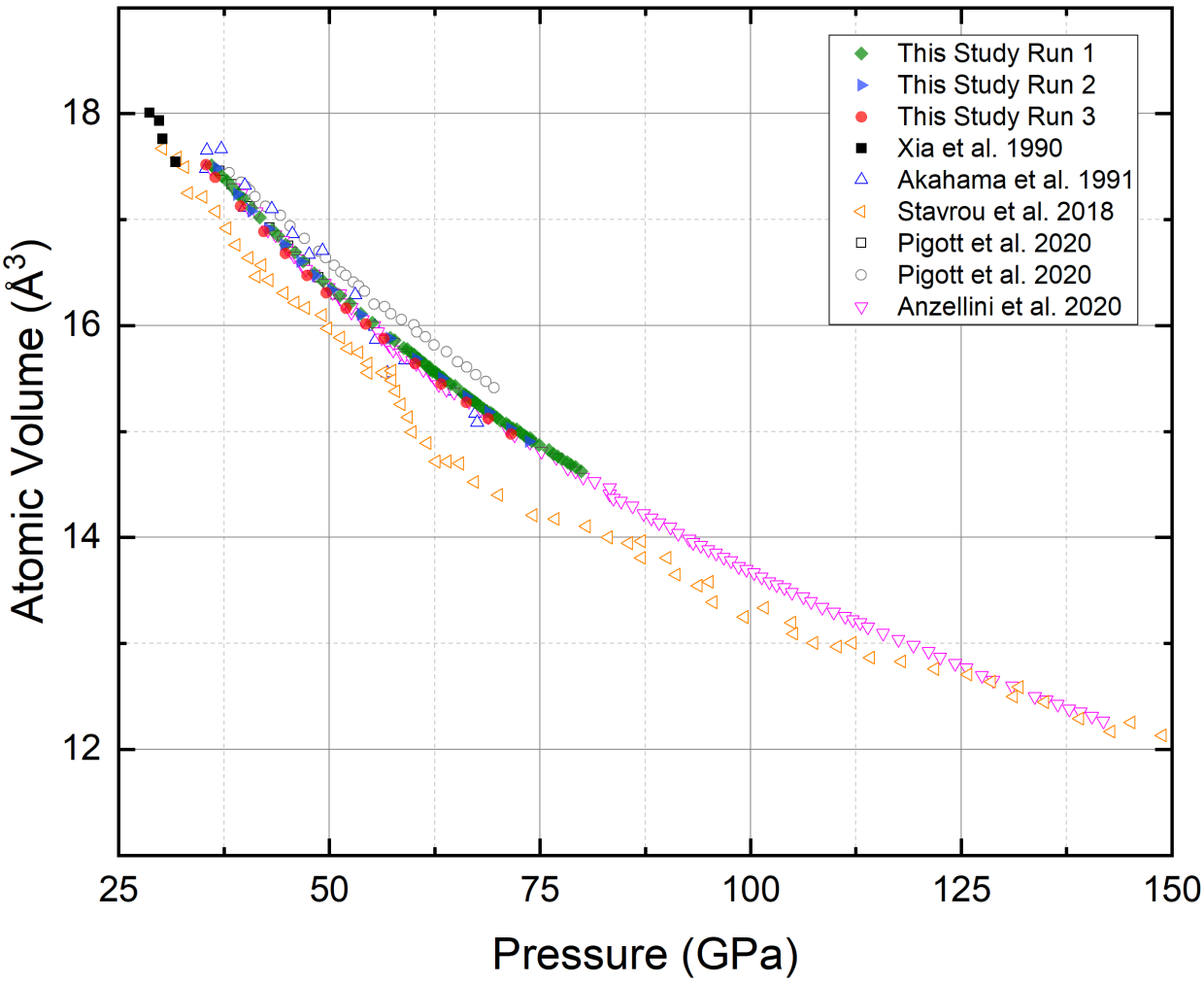

Figure 1. Pressure volume data for β-Zr from all three runs collected at room temperature in this study and Refs. [5,23-25,42].

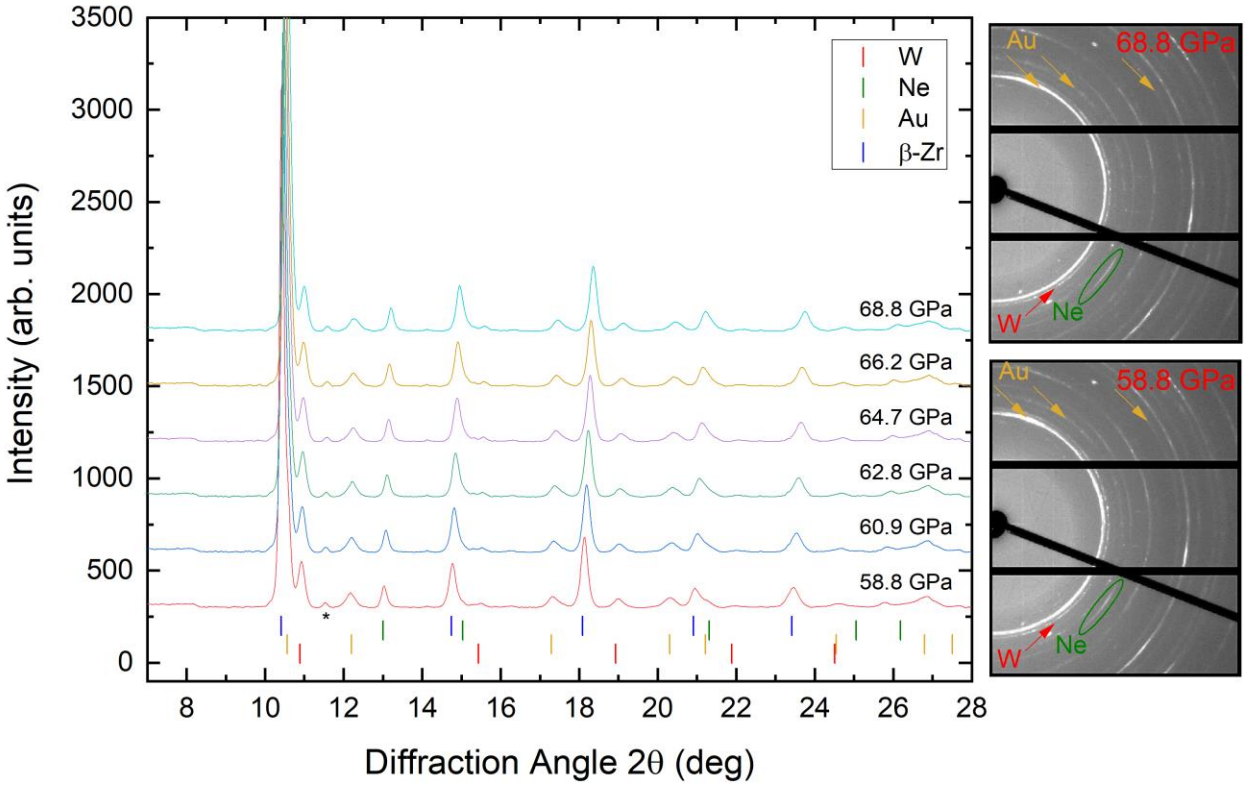

Figure 2. Integrated diffraction patterns and raw images from run 1 specifically in the pressure region of the proposed isostructural β → β' transition. The ticks correspond to predicted diffraction angles for β-Zr, Au, Ne, and W.

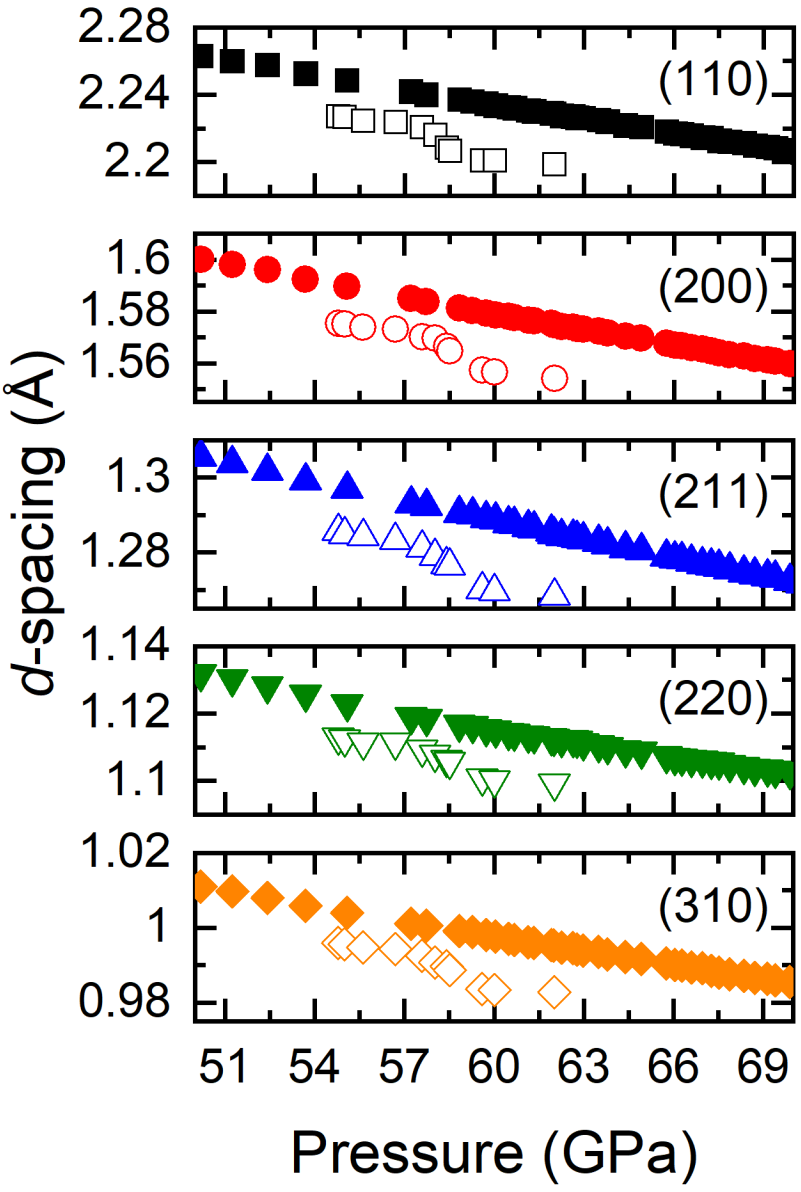

Figure 3. *d*-spacings as a function of pressure from run 1, no discontinuities are observed in the 57.5 to 60 GPa range. The report results of Stavrou et al. [23] are shown as open symbols and plot below our results showing that all their observed reflections are systematically shifted to lower *d*-spacings relative to ours.

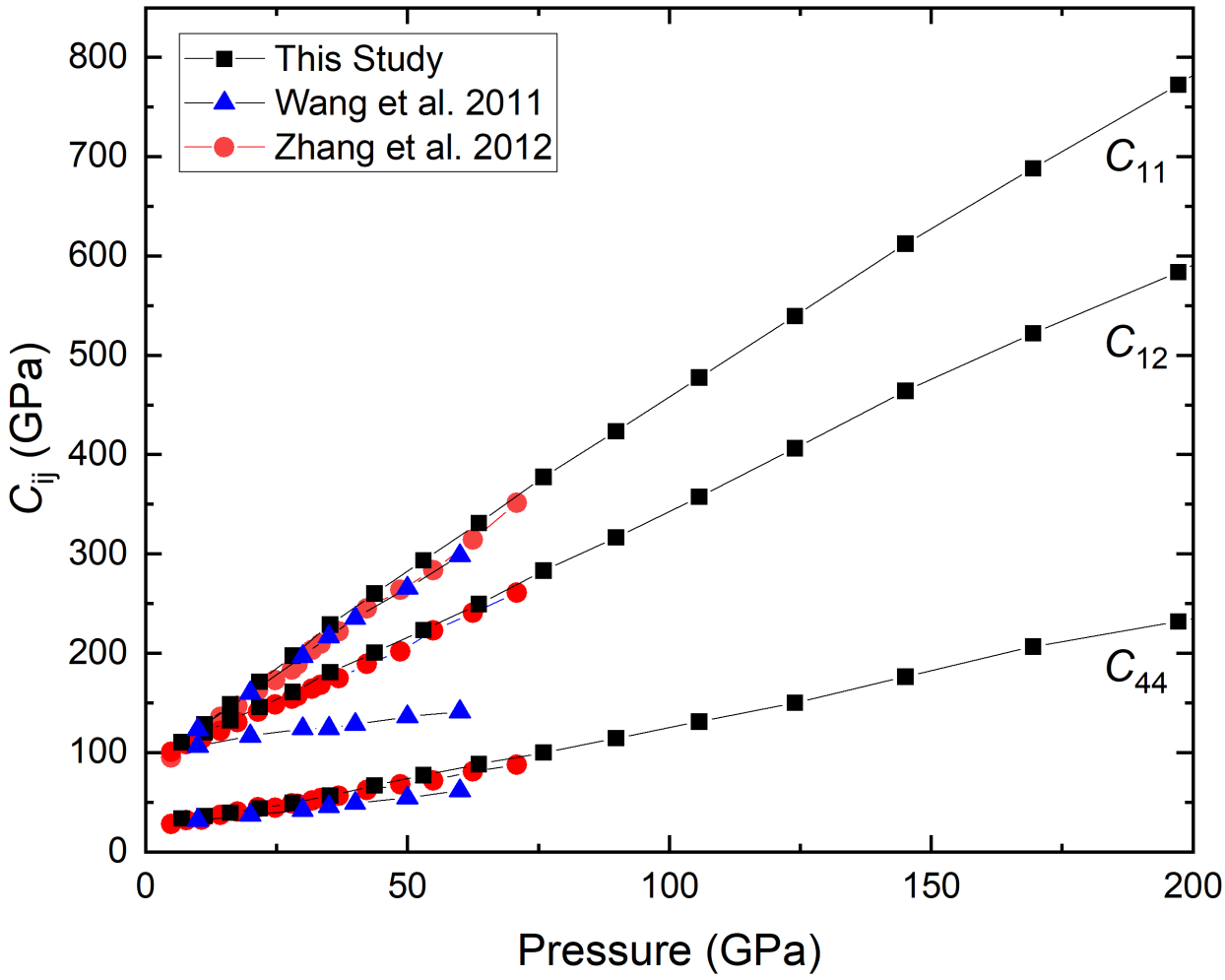

Figure 4. Calculated elastic constants of β-Zr plotted with plotted with [9,10]. Note that discontinuities are not observed in the pressure range of the proposed β → β‘ (57.5-60 GPa) or β‘ → β“ (110 GPa). Plots were limited to 200 GPa to facilitate an easy comparison to previous studies and calculated values up to 717 GPa are shown in table 4.

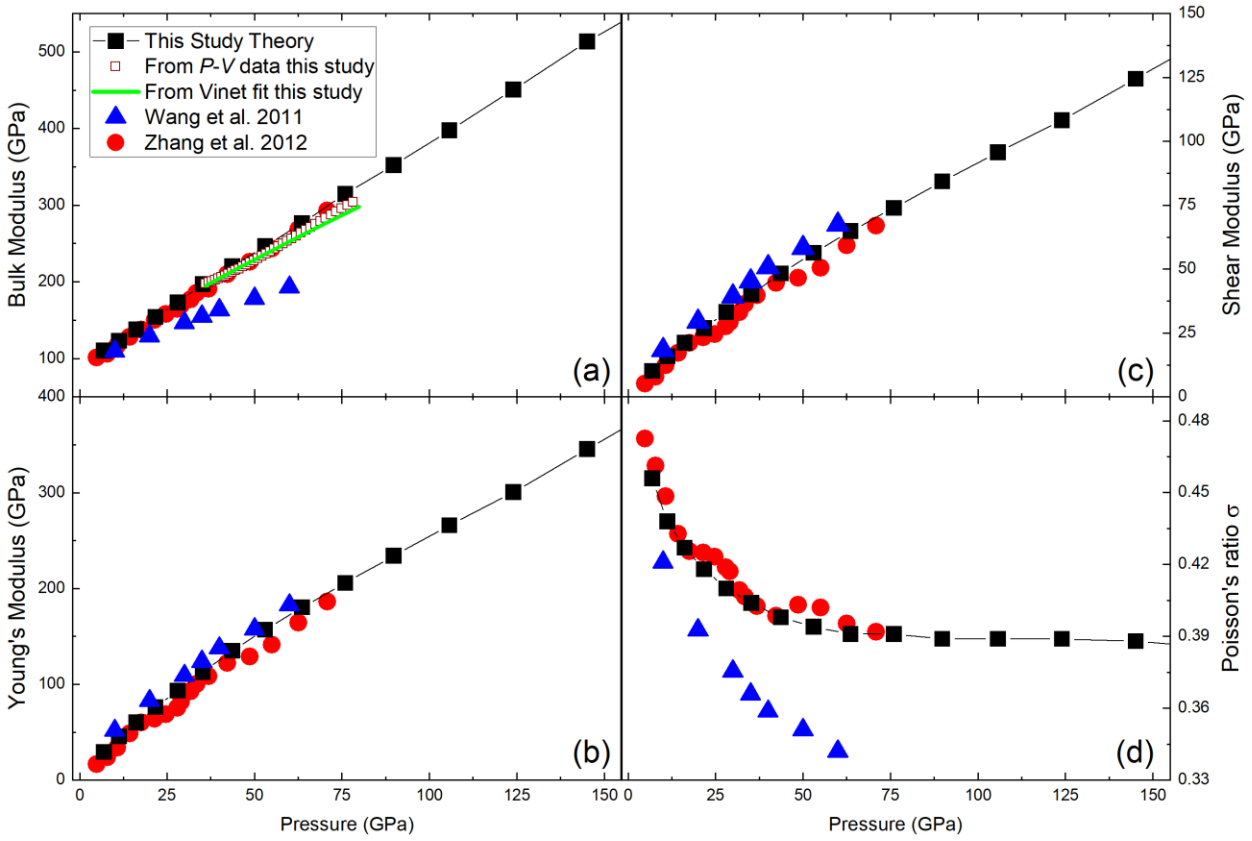

Figure 5. High-pressure (a) bulk modulus, (b) Young's modulus, (c) shear modulus, and (d) Poisson's ratio plotted together with the results from [9,10]. In (a) we also plot experimental results from run 1 calculated using two different approaches. Plots were limited to 150 GPa to facilitate an easy comparison to previous studies and calculated values up to 717 GPa are shown in table 4.

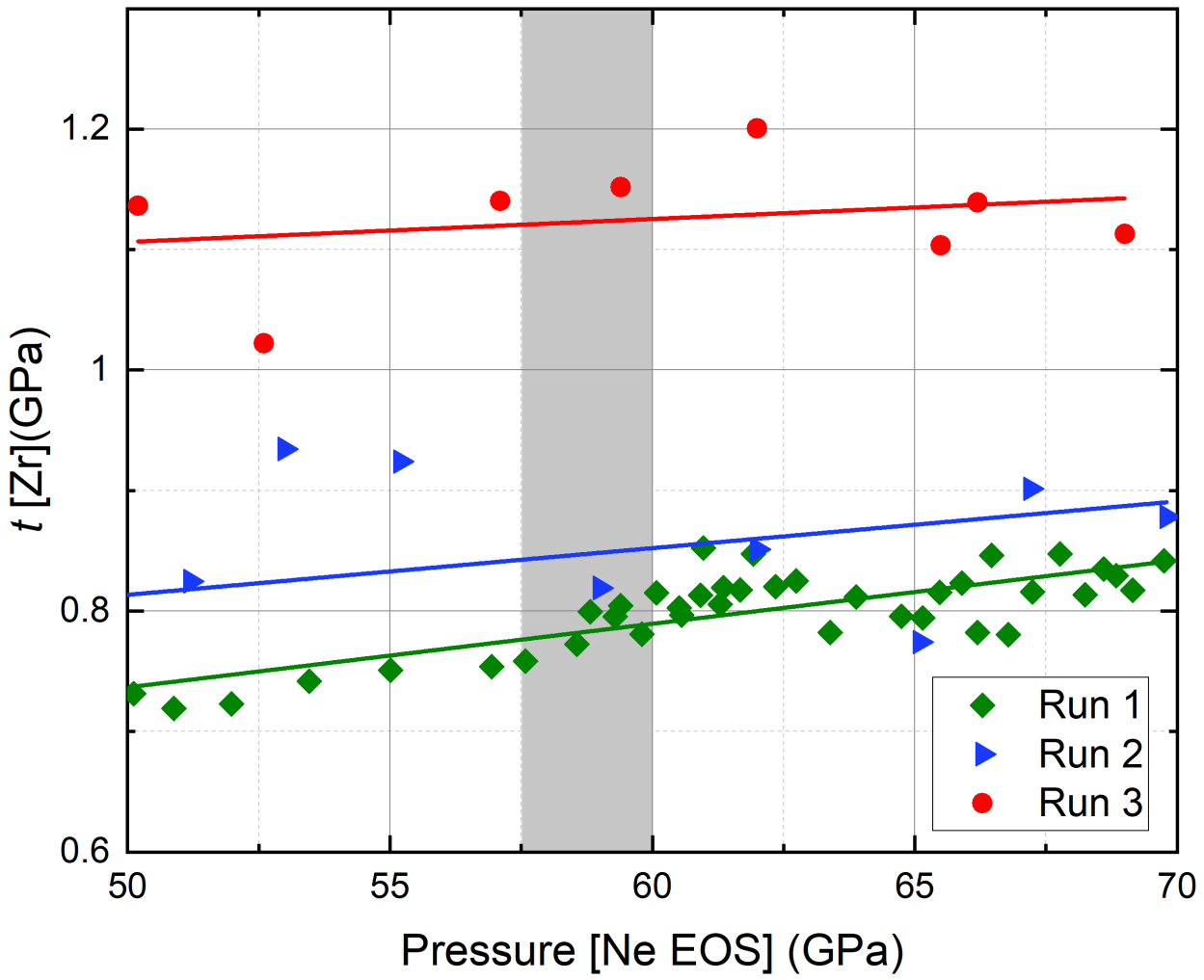

Figure 6. Uniaxial stress of β-Zr from 50 to 70 GPa from all three runs. Note that run 3 plots higher than both run 1 and 2 indicating that the pressurizing conditions in the Ne PTM were different that in this run. Overall, the uniaxial stress increases as pressure increases which is expected but it remains very low in these experiments and there are no discontinuities observed. Grey box indicates the pressure region of the isostructural phase transition proposed by Stavrou et al. [23].

Reference	Max pressure (GPa)	Zr purity (%)	α → ω (GPa)	ω → β (GPa)
This Study Run 1	79.9	99.94	10.7	34.9
This Study Run 2	73.7	99.9	10.8	35.0
This study Run 3	71.4	99.2	12.7	34.6
Akahama et al. [5]	68	99.8	6.7	33
Stavrou et al. [23]	211	99.5	12.7	30
Pigott et al. [24]	70	*Zr_0	-	35-37
Anzellini et al. [25]	142	99.2	14	35
Anzellini et al. [25]	142	98.8	20	35

Table 1. Max pressure, Zr purity and transition pressure for the α → ω and ω → β for all three runs and previous studies. For our three runs the reported pressure where the first evidence of the high-pressure phase is observed (so where the transition initiates). *Ultrapure zirconium see Rigg et al. [58] for impurities concentrations. Note Pigott et al. [24] did not report the pressure of the α → ω transition.

Run 1		Run 2		Run 3	
Pressure (GPa)	β-Zr Atomic Volume (Å^3)	Pressure (GPa)	β-Zr Atomic Volume (Å^3)	Pressure (GPa)	β-Zr Atomic Volume (Å^3)
36.0	17.514	36.6	17.487	35.3	17.521
36.6	17.472	39.0	17.240	36.4	17.400
37.2	17.411	40.7	17.082	39.4	17.130
37.9	17.368	42.7	16.917	42.2	16.889
38.6	17.294	44.6	16.765	44.8	16.684
39.2	17.240	46.5	16.608	47.3	16.475
39.8	17.200	48.3	16.472	49.6	16.313
40.7	17.112	50.2	16.338	52.0	16.166
41.8	17.023	53.7	16.105	54.3	16.017
43.2	16.909	57.1	15.883	56.4	15.879
43.9	16.851	60.3	15.688	60.2	15.645
44.8	16.766	63.4	15.505	63.2	15.451
45.9	16.694	66.3	15.332	66.2	15.277
46.9	16.609	68.9	15.184	68.8	15.125
48.2	16.495	71.4	15.030	71.6	14.978
49.2	16.423	73.7	14.908		
50.2	16.348				
51.3	16.285				
52.4	16.212				
53.7	16.115				
55.1	16.030				
57.2	15.887				
57.7	15.864				
58.8	15.792				
59.3	15.781				
59.7	15.738				
60.0	15.727				
60.5	15.693				
60.7	15.684				
61.1	15.651				
61.3	15.641				
61.9	15.607				
62.0	15.585				
62.3	15.568				
62.6	15.561				
62.8	15.548				
63.0	15.535				
63.5	15.508				

Continued on next page

Table 3 – continued from previous page	
63.8	15.484
64.4	15.450
64.9	15.431
65.8	15.368
66.0	15.352
66.3	15.341
66.6	15.322
67.0	15.297
67.3	15.283
67.5	15.268
67.9	15.245
68.4	15.216
68.7	15.194
69.1	15.180
69.4	15.165
69.9	15.132
70.3	15.108
71.0	15.075
71.3	15.059
71.8	15.031
72.2	15.021
72.7	14.992
73.2	14.964
73.4	14.950
73.9	14.939
74.1	14.912
74.9	14.875
76.1	14.828
76.6	14.790
77.1	14.765
77.6	14.742
78.3	14.710
78.7	14.689
79.2	14.665
79.9	14.626

Table 2. Pressures and volumes for β-Zr for all three runs. Pressure estimated from Ne (111) reflection using the calibration reported by [30].

Reference	V_0 (Å^3)	K_0 (GPa)	K'_0	Pressure range (GPa)
This study run 1	**22.6**	95.4(3)	3.15(2)	35-80
This study run 2	**22.6**	95.1(8)	3.13(4)	35-74
This study run 3	**22.6**	91.8(7)	3.25(5)	35-71
Stavrou et al. [23]	**22.6**	80(5)	3.35(40)	30-57.5
Pigott et al. [24]	**22.6**	105(1)	2.5(1)	35-50
Anzellini et al. [25]	**22.6**	93(1)	3.20(9)	35-142

Table 3. Vinet equation of state parameters obtained from fits to all three runs and found in the literature [23,25]. The bold values have been fixed during the fit.

Pressure (GPa)	Atomic Volume (Å^3)	C_{11} (GPa)	C_{12} (GPa)	C_{44} (GPa)	Bulk Modulus (GPa)	Shear Modulus (GPa)	Youngs Modulus (GPa)	Poisson's Ratio
6.9	21.112	110.4	110.4	33.7	110.4	10.1	29.5	0.456
11.2	20.340	128.5	120.6	36.1	123.2	15.9	45.7	0.438
16.2	19.586	148.4	132.4	39.5	137.7	21.1	60.3	0.427
21.7	18.852	171.4	145.7	43.9	154.3	26.9	76.2	0.418
28.1	18.136	197.6	161.0	49.3	173.2	33.1	93.4	0.41
35.2	17.439	228.8	180.9	56.8	196.9	40.2	112.8	0.404
43.7	16.759	260.1	200.8	66.9	220.6	48.3	135.0	0.398
53.0	16.098	293.6	223.2	77.2	246.6	56.3	157.0	0.394
63.6	15.454	331.2	249.4	88.4	276.7	64.9	180.5	0.391
76.0	14.828	377.5	283.1	100.0	314.6	74.0	205.7	0.391
89.8	14.218	423.5	316.6	114.4	352.2	84.3	234.3	0.389
105.7	13.626	477.5	357.6	131.1	397.6	95.7	265.9	0.389
124.0	13.050	539.4	406.4	150.0	450.7	108.2	300.6	0.389
145.1	12.491	612.2	464.1	176.3	513.5	124.5	345.6	0.388
169.5	11.948	688.2	522.2	206.7	577.5	143.4	397.2	0.385
197.2	11.421	772.4	583.7	232.0	646.6	161.7	447.8	0.385
229.2	10.910	884.5	668.2	261.2	740.3	183.4	508.2	0.386
266.7	10.414	1039.6	789.6	300.0	872.9	211.2	586.2	0.388
311.3	9.933	1229.6	939.6	356.8	1036.3	248.6	690.7	0.389
365.1	9.468	1430.3	1095.3	422.7	1207.0	291.6	809.7	0.388
430.1	9.017	1721.1	1331.1	511.6	1461.1	347.6	966.1	0.39
509.0	8.581	2055.5	1595.5	632.2	1748.9	421.7	1170.9	0.388
603.8	8.159	2383.1	1855.7	796.5	2031.5	512.0	1416.8	0.384
717.1	7.751	2759.0	2160.4	959.5	2360.0	602.6	1666.0	0.382

Table 4. Calculated atomic volume, elastic moduli, and Poisson's ratio for β-Zr